Mechanistic Insight Gained into the Ligand Substitution Reactions of Bis(*o*-benzosemiquinonediiminato)(triphenylphosphane)cobalt(III) – Kinetic, Solvent, and Volume Profile Studies

Basam M. Alzoubi,[a] Mohamed S. A. Hamza,[a][‡] Carlos Dücker-Benfer,[a] and Rudi van Eldik*[a]

Keywords: Cobalt / Kinetics / Ligand substitution / Mechanism / Pressure dependence / Solvent effects

The ligand substitution reactions of bis(*o*-benzosemiquinonediiminato)(triphenylphosphane)cobalt(III), $[Co^{III}(s\text{-}BQDI)_2(Ph_3P)]^+$, were studied with imidazole (Imid) and 4-dimethylaminopyridine (4-Me_2Npy) as entering nucleophiles in MeOH and CH_3CN as solvents (S). The complex $[Co^{III}(s\text{-}BQDI)_2(Ph_3P)S]^+$ undergoes dissociation of the solvent to form a five-coordinate intermediate, $[Co^{III}(s\text{-}BQDI)_2(Ph_3P)]^+$, which binds the entering nucleophile in a rate-determining step through a six-coordinate transition state, $[Co^{III}(s\text{-}BQDI)_2(Ph_3P)L]^+$, followed by the release of triphenylphosphane to form $[Co^{III}(s\text{-}BQDI)_2L]^+$. From the temperature and pressure dependence of the substitution of triphenylphosphane by imidazole, the activation parameters for the forward and reverse reactions of $[Co^{III}(s\text{-}BQDI)_2(Ph_3P)]^+$ with imidazole in MeOH were found to be $\Delta H^{\ddagger}$ = 58±2 and 43.4±0.5 kJ·mol^{-1}, $\Delta S^{\ddagger}$ = −116±6 and −73±2 J·K^{-1}·mol^{-1}, and $\Delta V^{\ddagger}$ = −10.6±0.1 and −8.7±0.3 cm^3·mol^{-1}, respectively. In CH_3CN, however, $\Delta H^{\ddagger}$, $\Delta S^{\ddagger}$, and $\Delta V^{\ddagger}$ for the forward reaction were found to be 50±3 kJ·mol^{-1}, −111±9 J·mol^{-1}·K^{-1}, and −12.9±0.3 cm^3·mol^{-1}, respectively. The activation parameters for the reaction between $[Co^{III}(s\text{-}BQDI)_2(Ph_3P)]^+$ and 4-dimethylaminopyridine in MeOH for the forward and reverse reactions were found to be $\Delta H^{\ddagger}$ = 76±2 and 47.9±0.4 kJ·mol^{-1}, $\Delta S^{\ddagger}$ = −51±7 and −64±2 J·K^{-1}·mol^{-1}, and $\Delta V^{\ddagger}$ = −10.5±0.3 and −11.1±0.2 cm^3·mol^{-1}, respectively. From these reported rate and activation parameters, the substitution of triphenylphosphane by imidazole and 4-dimethylaminopyridine follows an associative mechanism. The ligand substitution reactions of $[Co^{III}(s\text{-}BQDI)_2(Ph_3P)]^+$ in CH_3CN were found to be faster than those in MeOH, which is attributed to the potential for hydrogen bond formation with the entering nucleophile in the case of MeOH as solvent.

Introduction

The chemistry of transition metal complexes of benzosemiquinonediimine (s-BQDI), derived from *o*-phenylenediamine (OPD), are rather important because of their interesting redox properties[1,2] and their relation to biologically relevant catechol and benzoquinone derivatives.[3]

The bidentate ligand *o*-benzosemiquinonediiminato(−1), derived from the one-electron oxidation of *o*-phenylenediamine, can be stabilised by complex formation.[4] By removal of a second electron it is converted into the unstable *o*-benzoquinonediimine (BQDI) [Equation (1)], which can also be stabilised through complexation.[2]

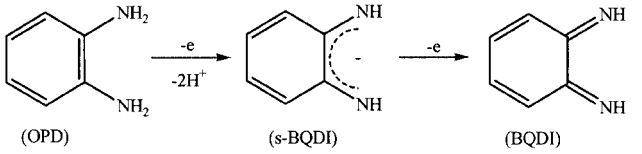

(1)

X-ray diffraction shows that the structure of $[Co^{III}(s\text{-}BQDI)_2(Ph_3P)]ClO_4$ is square-pyramidal in the solid state, with PPh_3 occupying one of the axial positions.[5] Upon dissolution in a coordinating solvent such as MeOH, the sixth position becomes occupied by a weakly bound solvent molecule, which cannot be observed in the solid-state structure.[3,6] Complexes such as $[Co^{III}(s\text{-}BQDI)_2(Ph_3P)]PF_6$, $[Co^{III}(s\text{-}BQDI)_2I]$, $[Co^{III}(s\text{-}BQDI)_2SCN]$, or $[Fe(s\text{-}BQDI)_2(Ph_3P)]$ are potentially five-coordinate in CH_3CN as solvent.[2]

We are interested generally in equilibria between five- and six-coordinate species in such complexes, since this should provide a better understanding of their mechanistic behaviour in ligand displacement processes. Alkyl cobalamines and cobinamides (vitamin B_{12} derivatives) with stronger donor ligands (e.g., vinyl, methyl, sulfite, dialkyl phosphite) exist as temperature-dependent mixtures of yellow five-coordinate and red six-coordinate aqua (solvent) complexes. Increasing the temperature favours the five-coordinate form with diethyl phosphite as ligand, whereas increasing the

[a] Institute for Inorganic Chemistry, University of Erlangen-Nürnberg,
Egerlandstr. 1, 91058 Erlangen, Germany
[‡] On leave from: Department of Chemistry, Ain Shams University, Cairo, Egypt

Supporting information for this article is available on the WWW under http://www.eurjic.org or from the author.

  DOI: 10.1002/ejic.200300107

pressure favours the six-coordinate form.[7] The reaction volume for the formation of the six-coordinate species in water as solvent was found to be $-12.5\ cm^3\ mol^{-1}$, suggesting that the entering water molecule is fully bound in the six-coordinate complex.[7]

The ligand substitution reactions of $[Co^{III}(s\text{-}BQDI)_2L]^+$, where L = Ph_3Sb and Ph_3As, and of $[Co^{III}(s\text{-}CBQDI)_2(Ph_3As)]^+$, where s-CBQDI = 4,5-dichloro-1,2-benzosemiquinonediiminato, were studied in methanol with different nucleophiles such as pyridine, pyrrolidine, and imidazole as entering ligands.[3,6] It was found that these nucleophiles easily displace the coordinated solvent molecule to form the six-coordinate $[Co^{III}(s\text{-}BQDI)_2LL']^+$ complexes, where L′ represents the entering nucleophile.[3] In a subsequent step, substitution of L by the entering nucleophile takes place, and an associative interchange mechanism was suggested.

In this investigation we performed a detailed analysis of the axial ligand substitution reactions of $[Co^{III}(s\text{-}BQDI)_2(Ph_3P)S]^+$ by imidazole and 4-$(Me)_2$Npy, where S is MeOH or CH_3CN, in order to study the intimate nature of the ligand displacement mechanism and the effect of the selected solvent on these reactions.

Results and Discussion

We started our studies by investigating the effect of temperature and pressure on the UV/Vis spectra of $[Co^{III}(s\text{-}BQDI)_2(Ph_3P)]^+$ in methanol as solvent. The UV/Vis spectrum of $5\cdot10^{-5}$ M $[Co^{III}(s\text{-}BQDI)_2(Ph_3P)]^+$ was recorded as a function of temperature, as shown in Figure S-1 (Supporting Information). With decreasing temperature, from 60 to 5 °C, it exhibits isosbestic points at 508, 600, and 760 nm, a significant absorbance decrease at 712 and 450 nm, and an increase in absorbance at 550 nm. Similar spectra were obtained either on decreasing the temperature or on increasing the pressure.

The effect of temperature and pressure on the UV/Vis spectra suggests an equilibrium between five- and six-coordinate forms of the complex $[Co^{III}(s\text{-}BQDI)_2(Ph_3P)S]^+$, where the sixth coordination site is occupied by a solvent molecule. The six-coordinate form is favoured by increasing pressure or decreasing temperature, and vice versa for the five-coordinate complex. Similar trends could be observed in both solvents (MeOH and CH_3CN). In the case of CH_3CN as solvent, however, the change in the UV/Vis spectrum was not as significant as in that of MeOH as solvent, which is attributed to the fact that CH_3CN is a much stronger nucleophile than MeOH and will form a less labile six-coordinate species. For this reason a smaller fraction of the five-coordinate species will exist in equilibrium with the six-coordinate species in the case of CH_3CN as solvent. In the solid state the complex is square-pyramidal with a Ph_3P ligand occupying the axial position.[5]

Reaction between $[Co^{III}(s\text{-}BQDI)_2(Ph_3P)]^+$ and Imidazole in Methanol

The UV/Vis spectrum of $[Co^{III}(s\text{-}BQDI)_2(Ph_3P)]^+$ exhibits two bands at 710 and 478 nm, with a shoulder at 423 nm ($\varepsilon = 2.2\cdot10^4$, $1.1\cdot10^4$, and $7.9\cdot10^3\ M^{-1}\cdot cm^{-1}$, respectively). Upon mixing of the complex with imidazole or 4-$(Me)_2$Npy in the stopped-flow instrument, there is a small and very rapid initial increase in absorbance prior to the reaction with the entering nucleophile. This rapid increase can be ascribed to a fast equilibration between the complex and the solvent (methanol) as a result of the equilibrium between the five- and six-coordinate complexes in solution as discussed above. This rapid absorbance change is also observed in the absence of imidazole or 4-$(Me)_2$Npy, just by dilution of a solution of the complex with solvent in a stopped-flow instrument, and occurs within the mixing time of the instrument (2 ms) at room temperature. With the use of a Biologic low temperature stopped-flow unit, however, the spectral changes associated with this reaction could be recorded at −40 °C, and a typical kinetic trace (see Figure S-2, Supporting Information) indicates that this reaction is over within 2 s at −40 °C. Subsequently, there is a much larger absorbance decrease at 710 and 450 nm, and an increase at 540 nm, associated with the coordination of imidazole. The $[Co^{III}(s\text{-}BQDI)_2(Imid)]^+$ complex shows two bands at 716 and 496 nm, with a shoulder at 420 nm ($\varepsilon = 1.1\cdot10^5$, $5.7\cdot10^4$, and $3.9\cdot10^4\ M^{-1}\cdot cm^{-1}$, respectively), whereas $[Co^{III}(s\text{-}BQDI)_2(4\text{-}Me_2Npy)]^+$ has characteristic UV/Vis bands at 714 and 520 nm, with a shoulder at 422 nm ($\varepsilon = 6.7\cdot10^4$, $5.2\cdot10^4$, and $3.1\cdot10^4\ M^{-1}\cdot cm^{-1}$, respectively).

The reaction between $2.5\cdot10^{-5}$ M $[Co^{III}(s\text{-}BQDI)_2(Ph_3P)]^+$ and an excess of imidazole (0.05 to 1.0 M) was studied in methanol as a function of temperature (15−45 °C). Kinetic traces for this reaction revealed perfect pseudo-first order behaviour, and the kinetic results as a function of the imidazole concentration are shown in Figure 1. It follows that good linear plots with significant intercepts are obtained within the experimental error limits. Furthermore, the plots do not indicate any saturation at high [Imid]. This kinetic behaviour can be expressed by the rate law given in Equation (2), where k_a and k_b represent the rate constants for the forward (slope) and reverse (intercept) reactions, respectively. Values of k_a and k_b as a function of temperature, along with the corresponding activation parameters, are summarised in Table 1. Values of $\Delta H^{\ddagger}$ and $\Delta S^{\ddagger}$ for the forward reaction (k_a) were found to be $58\pm2\ kJ\cdot mol^{-1}$ and $-116\pm6\ J\cdot K^{-1}\cdot mol^{-1}$, whereas those for the reverse reaction (k_b) were found to be $68\pm1\ kJ\cdot mol^{-1}$ and $-82\pm3\ J\cdot K^{-1}\cdot mol^{-1}$, respectively.

$$k_{obsd.} = k_a[L] + k_b \quad (2)$$

The results in Figure 1 clearly indicate that we are dealing with an unfavourable displacement of triphenylphosphane by imidazole, as can be seen from the magnitude of the intercepts of the plots that represent the contribution of the reverse reaction. Under the selected experimental conditions (no free phosphane added), the reverse displacement of imidazole by phosphane will follow second-order kinetics, with the result that the kinetic data measured under

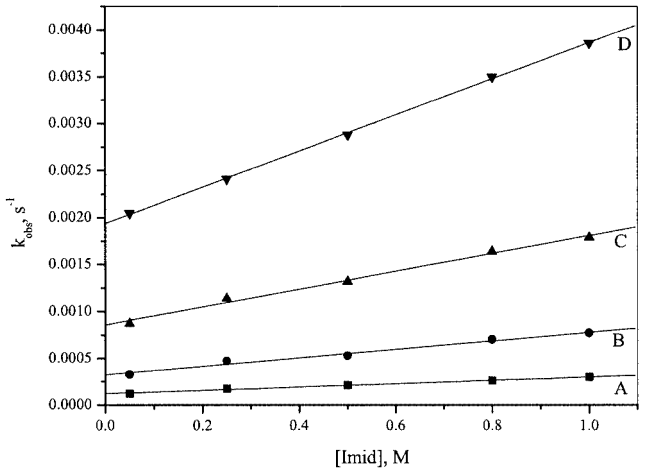

Figure 1. Plots of $k_{obsd.}$ versus [Imid] for the reaction between $[Co^{III}(s\text{-}BQDI)_2(Ph_3P)]^+$ and imidazole in methanol as a function of temperature; experimental conditions: $[Co^{III}] = 2.5\cdot10^{-5}$ M, temperature: 15.0 (A), 25.0 (B), 35.0 (C), 45.0 °C (D)

Table 1. Kinetic data for the reaction between $[Co^{III}(s\text{-}BQDI)_2(Ph_3P)]^+$ and imidazole in the absence of added phosphane in methanol as a function of temperature and pressure $\{[Co^{III}(s\text{-}BQDI)_2(Ph_3P)]^+ = 2.5\cdot10^{-5}$ M$\}$

$$[Co^{III}(s\text{-}BQDI)_2(Ph_3P)]^+ + Imid \underset{k_b}{\overset{k_a}{\rightleftharpoons}} [Co^{III}(s\text{-}BQDI)_2(Imid)]^+ + Ph_3P$$

Pressure, MPa	Temp., °C	$k_a \times 10^4$, $M^{-1}\,s^{-1}$	$k_b \times 10^4$, s^{-1} [a]
0.1	15.0	1.79±0.08	1.21±0.05
	25.0	4.5±0.3	3.2±0.2
	35.0	9.5±0.5	8.6±0.3
	45.0	19.3±1.4	19.4±0.8
10	15.0	2.39±0.06	1.30±0.04
50		2.85±0.01	1.47±0.01
90		3.41±0.08	1.63±0.05
130		4.06±0.10	1.87±0.07
$\Delta H^{\ddagger}$, $kJ\cdot mol^{-1}$		58±2	68±1
$\Delta S^{\ddagger}$, $J\cdot K^{-1}\cdot mol^{-1}$		−116±6	−82±3
$\Delta V^{\ddagger}$, $cm^3\cdot mol^{-1}$		−10.6±0.1	−7.2±0.3

[a] First-order rate constant obtained from the intercept of plots of $k_{obsd.}$ versus [Imid].

pseudo-first order conditions at low imidazole concentrations could become unreliable due to a contribution of the second-order reverse process. We therefore studied the rate and activation parameters for the reverse substitution of imidazole by Ph_3P separately, by first treating $2.5\cdot10^{-4}$ M of $[Co^{III}(s\text{-}BQDI)_2(Ph_3P)]^+$ with 1 M imidazole to form the imidazole complex, followed by the addition of an excess of Ph_3P to form the $[Co^{III}(s\text{-}BQDI)_2(Ph_3P)]^+$ complex again. Figure 2 shows a linear plot of $k_{obsd.}$ versus $[Ph_3P]$ for the reaction between $[Co^{III}(s\text{-}BQDI)_2(Imid)]^+$ and an excess of Ph_3P (0.005−0.025 M). The linear plot exhibits a negligible intercept, indicating that the displacement of imidazole by phosphane goes to completion under the selected conditions. The slope of the line in Figure 2 represents k_b, for which the results are reported as a function of temperature

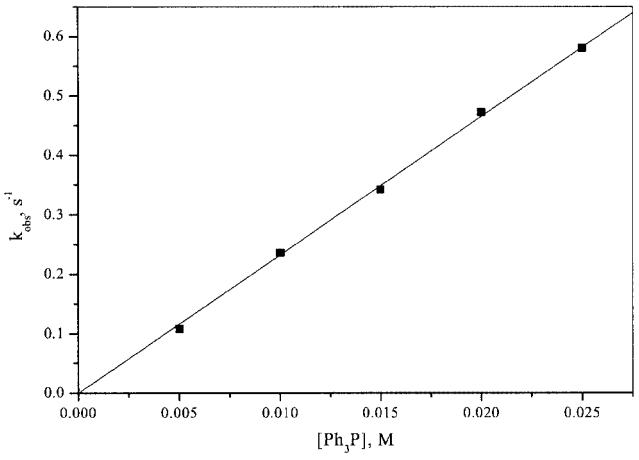

Figure 2. Plot of $k_{obsd.}$ versus $[Ph_3P]$ for the reaction between $1.25\cdot10^{-4}$ M $[Co^{III}(s\text{-}BQDI)_2(Imid)]^+$ and Ph_3P in methanol at 25 °C; the best fit (solid line) gives $k_b = 23.3\ M^{-1}\cdot s^{-1}$

Table 2. Kinetic data for the reaction between $[Co^{III}(s\text{-}BQDI)_2(Imid)]^+$ and Ph_3P in methanol as a function of temperature and pressure

$$[Co^{III}(s\text{-}BQDI)_2(Imid)]^+ + Ph_3P \underset{k_b}{\overset{k_a}{\rightleftharpoons}} [Co^{III}(s\text{-}BQDI)_2(Ph_3P)]^+ + Imid$$

Pressure, MPa	Temp., °C	$k_b/[Ph_3P]$, $M^{-1}\,s^{-1}$ [a]
0.1	5.0	6.2±0.3[b]
	10.0	8.8±0.2[b]
	15.0	12.5±0.1[b]
	20.0	17.2±0.3[b]
	25.0	23.2±0.1[b]
10	25.0	23.6±0.6[c]
50		26.9±0.3[c]
90		30.7±2.0[c]
130		36.0±1.5[c]
$\Delta H^{\ddagger}$, $kJ\cdot mol^{-1}$		43.4±0.5
$\Delta S^{\ddagger}$, $J\cdot K^{-1}\cdot mol^{-1}$		−73±2
$\Delta V^{\ddagger}$, $cm^3\cdot mol^{-1}$		−8.7±0.3

[a] Second-order rate constant calculated from the slope of plots of k_b versus $[Ph_3P]$. [b] $[Co^{III}(s\text{-}BQDI)_2(Imid)]^+ = 1.25\cdot10^{-4}$ M, $[Ph_3P] = 2.5\cdot10^{-2}$ M. [c] $[Co^{III}(s\text{-}BQDI)_2(Imid)]^+ = 1.25\cdot10^{-4}$ M, $[Ph_3P] = 1.25\cdot10^{-2}$ M.

in Table 2. The $\Delta H^{\ddagger}$ and $\Delta S^{\ddagger}$ values for k_b were found to be 43.4±0.5 $kJ\cdot mol^{-1}$ and −73±2 $J\cdot K^{-1}\cdot mol^{-1}$, respectively.

The reaction between $2.5\cdot10^{-5}$ M $[Co^{III}(s\text{-}BQDI)_2(Ph_3P)]^+$ and imidazole ([Imid] = 0.05−1 M) was studied at different pressures (10−130 MPa). The results are shown in Figure 3, from which it follows that good linear plots with significant intercepts are obtained within the experimental error limits. The values of k_a and k_b as a function of pressure, along with the corresponding activation volumes, are summarised in Table 1. Plots of ln k_a and ln k_b versus pressure were linear within the error limits (Figures S-3 and S-4, Supporting Information), and values of $\Delta V^{\ddagger}$ for the forward and the reverse reactions were found to be −10.6±0.1 and −7.2±0.3 $cm^3\cdot mol^{-1}$, respectively.

Because of the possible unreliability of k_b under these conditions, as indicated above, its pressure dependence was also measured directly by treatment of the imidazole complex with an excess of phosphane, the results of which are included in Table 2. A plot of ln k_b versus pressure gave a good linear relationship, from which $\Delta V^{\ddagger}$ was calculated to be -8.7 ± 0.3 cm^3·mol^{-1}.

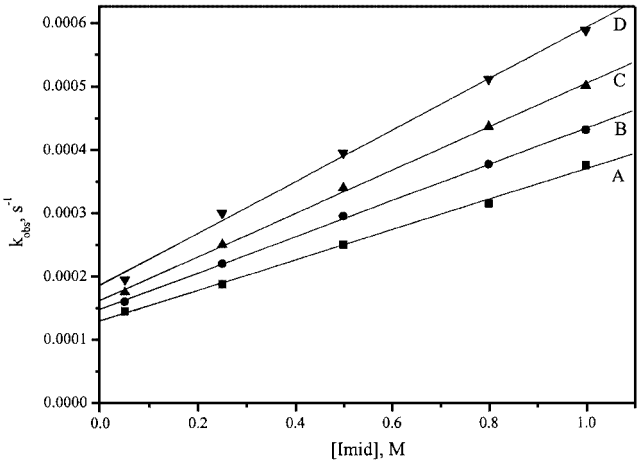

Figure 3. Plots of $k_{obsd.}$ versus [Imid] for the reaction between $[Co^{III}(s\text{-}BQDI)_2(Ph_3P)]^+$ and phosphane in methanol as a function of pressure; experimental conditions: $[Co^{III}] = 2.5\cdot10^{-5}$ M, pressure: 10 (A), 50 (B), 90 (C), 130 MPa (D)

From the available kinetic and spectroscopic data, we suggest that the reaction between $[Co^{III}(s\text{-}BQDI)_2(Ph_3P)S]^+$ and imidazole (or 4-Me_2Npy, see later) takes place in two consecutive steps. There is rapid dissociation of coordinated solvent in Equation (3) to form a five-coordinate intermediate, followed by the rate-determining associative ligand exchange process Equation (4) to form the product complex.

$$[Co^{III}(s\text{-}BQDI)_2(Ph_3P)S]^+ \rightleftarrows [Co^{III}(s\text{-}BQDI)_2(Ph_3P)]^+ + S \quad (3)$$

$$[Co^{III}(s\text{-}BQDI)_2(Ph_3P)]^+ + L \underset{k_b}{\overset{k_a}{\rightleftharpoons}} [Co^{III}(s\text{-}BQDI)_2(L)]^+ + PPh_3 \quad (4)$$

From the activation parameters and the constructed volume profile shown in Figure 4, it is reasonable to conclude that the reaction between $[Co^{III}(s\text{-}BQDI)_2(Ph_3P)]^+$ and imidazole in methanol follows an associative mechanism through the formation of a six-coordinate intermediate/transition state.

Reaction between $[Co^{III}(s\text{-}BQDI)_2(Ph_3P)]^+$ and 4-$(Me)_2$Npy in Methanol

The reaction between $2.5\cdot10^{-5}$ M $[Co^{III}(s\text{-}BQDI)_2(Ph_3P)]^+$ and an excess of 4-Me_2Npy (0.05 to 1 M) in methanol as a function of temperature (15−45 °C) was studied in a similar way. The results are presented in Figure S-5 (Supporting Information), from which it follows that good linear plots with significant intercepts are obtained

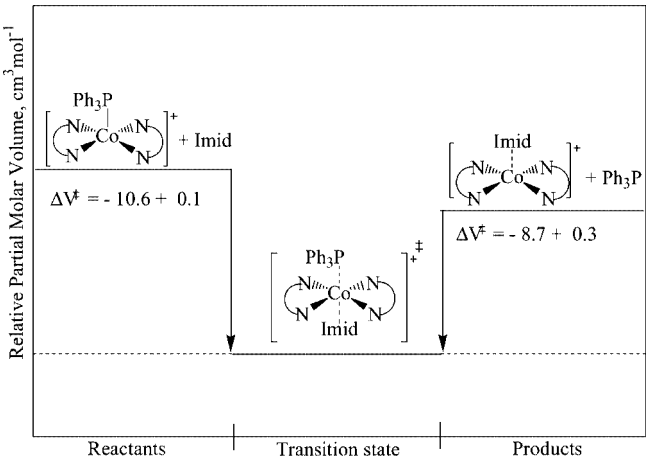

Figure 4. Volume profile for the reaction (the given structures are schematic presentations)

within the experimental error limits. Furthermore, the plots do not indicate any saturation at high 4-Me_2Npy concentrations. In this case the intercepts are smaller and the slopes of the plots larger than in the case of the reaction with imidazole, indicating that a more favourable equilibrium situation is reached in the reaction with 4-Me_2Npy. The same rate law and data treatment as used for the reaction with imidazole can be adopted, and the results are summarized as a function of temperature and pressure in Table 3. The values of $\Delta H^{\ddagger}$ and $\Delta S^{\ddagger}$ for the forward reaction (k_a) were found to be 76 ± 2 kJ·mol^{-1} and -51 ± 7 J·K^{-1}·mol^{-1}, respectively, and those for the reverse reaction to be 61 ± 4 kJ·mol^{-1} and -115 ± 12 J·K^{-1}·mol^{-1}, respectively. Because of the possible contribution of a second-order reverse reaction at low 4-Me_2Npy concentration, we also determined the rate and activation parameters for the substitution of 4-Me_2Npy by Ph_3P to form $[Co^{III}(s\text{-}BQDI)_2(Ph_3P)]^+$ directly, by treatment of $2.5\cdot10^{-4}$ M $[Co^{III}(s\text{-}BQDI)_2(Ph_3P)]^+$ with 1 M 4-Me_2Npy, followed by the reaction with phosphane. A plot of $k_{obsd.}$ versus $[Ph_3P]$ for the reaction between $[Co^{III}(s\text{-}BQDI)_2(4\text{-}Me_2Npy)]^+$ and excess Ph_3P (0.005−0.025 M) is shown in Figure S-6 (Supporting Information), from which it follows that the back reaction does not contribute significantly under these conditions. The data for k_b are summarised in Table 4. The values of $\Delta H^{\ddagger}$ and $\Delta S^{\ddagger}$ were found to be 47.9 ± 0.4 kJ·mol^{-1} and -64 ± 2 J·K^{-1}·mol^{-1}, respectively.

The reaction between $2.5\cdot10^{-5}$ M $[Co^{III}(s\text{-}BQDI)_2(Ph_3P)]^+$ and 4-Me_2Npy (0.05 to 1 M) as a function of pressure (10−130 MPa) was also studied, and the results are reported in Figure S-7 (Supporting Information). The data show good linear plots with significant intercepts within the experimental error limits. The values of k_a and k_b as a function of pressure, along with the corresponding activation parameters, are summarised in Table 3. Plots of lnk_a and lnk_b versus pressure gave good linear fits, from which the values of $\Delta V^{\ddagger}$ for the forward and reverse reactions were calculated to be -10.5 ± 0.3 and -8.7 ± 0.6

Table 3. Kinetic data for the reaction between $[Co(s\text{-}BQDI)_2(Ph_3P)]^+$ and 4-Me_2Npy in the absence of added phosphane in methanol as a function of temperature and pressure $\{[Co^{III}(s\text{-}BQDI)_2(Ph_3P)]^+ = 2.5\cdot10^{-5}$ M$\}$

$$[Co^{III}(s\text{-}BQDI)_2(Ph_3P)]^+ + 4\text{-}Me_2Npy \underset{k_b}{\overset{k_a}{\rightleftharpoons}} [Co^{III}(s\text{-}BQDI)_2(4\text{-}Me_2Npy)]^+ + Ph_3P$$

Pressure, MPa	Temp., °C	$k_a \times 10^4$, M^{-1} s^{-1}	$k_b \times 10^4$, s^{-1} [a]
0.1	15.0	2.5±0.2	0.54±0.02
	25.0	6.7±0.5	1.6±0.2
	35.0	19±1	3.1±0.2
	45.0	54±2	6.9±0.4
10	15.0	2.5±0.1	0.54±0.04
50		3.10±0.08	0.64±0.05
90		3.65±0.09	0.74±0.06
130		4.3±0.1	0.83±0.06
$\Delta H^{\ddagger}$, kJ·mol^{-1}		76±2	61±4
$\Delta S^{\ddagger}$, J·K^{-1}·mol^{-1}		−51±7	−115±12
$\Delta V^{\ddagger}$, cm^3·mol^{-1}		−10.5±0.3	−8.7±0.6

[a] First-order rate constant obtained from the intercept of plots of $k_{obsd.}$ versus [4-Me_2Npy].

Table 4. Kinetic data for the reaction between $[Co^{III}(s\text{-}BQDI)_2(4\text{-}Me_2Npy)]^+$ and Ph_3P in methanol as a function of temperature and pressure

$$[Co^{III}(s\text{-}BQDI)_2(4\text{-}Me_2Npy)]^+ + Ph_3P \underset{k_b}{\overset{k_a}{\rightleftharpoons}} [Co^{III}(s\text{-}BQDI)_2(Ph_3P)]^+ + 4\text{-}Me_2Npy$$

Pressure, MPa	Temp., °C	$k_b/[Ph_3P]$, M^{-1} s^{-1} [a]
0.1	5.0	2.8±0.1[b]
	10.0	4.2±0.1[b]
	15.0	6.0±0.1[b]
	20.0	8.6±0.1[b]
	25.0	12.1±0.1[b]
10	25.0	15.4±0.8[c]
50		18.6±1.6[c]
90		22.0±1.3[c]
130		26.5±1.1[c]
$\Delta H^{\ddagger}$, kJ·mol^{-1}		47.9±0.4
$\Delta S^{\ddagger}$, J·K^{-1}·mol^{-1}		−64±2
$\Delta V^{\ddagger}$, cm^3·mol^{-1}		−11.1±0.2

[a] Second-order rate constant calculated from the slope of plots of k_b versus $[Ph_3P]$. [b] $[Co^{III}(s\text{-}BQDI)_2(4\text{-}Me_2Npy)]^+ = 1.25\cdot10^{-4}$ M, $[Ph_3P] = 2.5\cdot10^{-2}$ M. [c] $[Co^{III}(s\text{-}BQDI)_2(4\text{-}Me_2Npy)]^+ = 1.25\cdot10^{-4}$ M, $[Ph_3P] = 1.25\cdot10^{-2}$ M.

cm^3·mol^{-1}, respectively. The values of k_b were also measured directly as a function of pressure, with use of the displacement of 4-Me_2Npy by phosphane, and a plot of $\ln k_b$ versus pressure resulting in a $\Delta V^{\ddagger}$ value of −11.1±0.2 cm^3·mol^{-1} (see Table 4). From the reported activation parameters, we can conclude that the reverse reaction between $[Co^{III}(s\text{-}BQDI)_2(Ph_3P)]^+$ and 4-$(Me)_2$Npy follows the same associative reaction mechanism, in which the entering nucleophile is coordinated to the Co^{III} centre in the six-coordinate intermediate/transition state.

The forward rate constants for the reaction between $[Co^{III}(s\text{-}BQDI)_2(Ph_3P)]$ and 4-$(Me)_2$Npy or imidazole are $6.7\cdot10^{-4}$ and $4.5\cdot10^{-4}$ $M^{-1}\cdot s^{-1}$ at 25 °C, respectively, whereas the rate constants for the reverse reactions are 12.1 and 23.2 $M^{-1}\cdot s^{-1}$ at 25 °C, respectively. This indicates that the forward rate constant (k_a) increases with increasing basicity of the entering ligand, whereas the reversible reaction rate constant (k_b) decreases with increasing basicity due to the stronger cobalt−ligand bond.

Reaction between $[Co^{III}(s\text{-}BQDI)_2(Ph_3P)]^+$ and Imidazole in Acetonitrile

The reaction between $2.5\cdot10^{-5}$ M $[Co^{III}(s\text{-}BQDI)_2(Ph_3P)]^+$ and excess imidazole ([Imid] = 0.025−1 M) in acetonitrile was studied at different temperatures (11−32 °C). The results are presented in Figure 5 and show a significant deviation from linearity at high imidazole concentrations, as well as negligible intercepts. This behaviour can be accounted for in terms of the interchange mechanism presented in reactions according to Equations (5) and (6), for which the rate law is given in Equation (7), where K represents the equilibrium constant for precursor formation, and k the interchange rate constant. Since acetonitrile is a much more strongly coordinating solvent than methanol, this presumably prevents formation of a five-coordinate intermediate and forces the reaction to proceed through an interchange instead of an associative mechanism involving a five-coordinate intermediate.

$$[Co^{III}(s\text{-}BQDI)_2(Ph_3P)S]^+ + Imid \rightleftarrows \{[Co^{III}(s\text{-}BQDI)_2(Ph_3P)S]^+\cdot Imid\};\ K \quad (5)$$

$$\{[Co^{III}(s\text{-}BQDI)_2(Ph_3P)S]^+\cdot Imid\} \rightarrow [Co^{III}(s\text{-}BQDI)_2(Imid)S]^+ + Ph_3P;\ k \quad (6)$$

$$k_{obs} = \frac{k\cdot K[Imid]}{\{1 + K[Imid]\}} \quad (7)$$

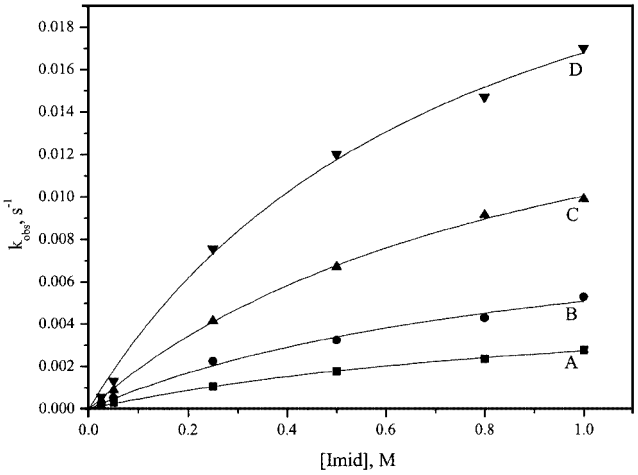

Figure 5. Plots of $k_{obsd.}$ versus [Imid] for the reaction between $[Co^{III}(s\text{-}BQDI)_2(Ph_3P)]^+$ and imidazole in acetonitrile as a function of temperature; experimental conditions: $[Co^{III}] = 2.5\cdot10^{-5}$ M, temperature: 11.0 (A), 18.0 (B), 25.0 (C), 32.0 °C (D)

Table 5. Kinetic data for the reaction between $[Co^{III}(s\text{-}BQDI)_2(Ph_3P)]^+$ and imidazole in acetonitrile as a function of temperature and pressure

Pressure, MPa	Temp., °C	$k{\cdot}K \times 10^3$, $M^{-1}\,s^{-1}$ [a]	K, M^{-1} [b]	$k \times 10^3$, s^{-1} [b]
0.1	11.0	5.8±0.1[c]	0.9±0.1	5.8±0.5
	18.0	10.4±0.5[c]	1.0±0.2	10±2
	25.0	18±4[c]	1.1±0.1	19±1
	32.0	26±2[c]	1.3±0.1	29±3
10	5.0	4.9±0.2[d]		
50		6.1±0.3[d]		
90		7.5±0.1[d]		
130		9.6±0.1[d]		
$\Delta H^{\ddagger}$, $kJ{\cdot}mol^{-1}$		50±3[c]		
$\Delta S^{\ddagger}$, $J{\cdot}mol^{-1}{\cdot}K^{-1}$		−111±9[c]		
$\Delta V^{\ddagger}$, $cm^3{\cdot}mol^{-1}$		−12.9±0.3[d]		

[a] $k{\cdot}K$ was calculated from $k_{obsd.}$/[Imid] at [Imid] = 0.05 M. [b] K and k were calculated from the nonlinear least-squaresfit by use of Equation (7). [c] $[Co^{III}(s\text{-}BQDI)_2(Ph_3P)]^+ = 2.5{\cdot}10^{-5}$ M. [d] $[Co^{III}(s\text{-}BQDI)_2(Ph_3P)]^+ = 2.5{\cdot}10^{-5}$ M, [Imid] = 0.025 M.

The values of k and K as a function of temperature were calculated from a nonlinear fit of the measured rate constants and are summarised, along with the corresponding activation parameters, in Table 5. The values of $\Delta H^{\ddagger}$ and $\Delta S^{\ddagger}$ for the overall reaction between $[Co^{III}(s\text{-}BQDI)_2(Ph_3P)]^+$ and imidazole in CH_3CN were calculated for $k{\cdot}K = k_{obsd.}$/[Imid] at [Imid] = 0.05 M (i.e., where the imidazole concentration dependence is still linear), and were found to be 50±3 $kJ{\cdot}mol^{-1}$ and −111±9 $J{\cdot}K^{-1}{\cdot}mol^{-1}$, respectively. The pressure dependence of the reaction was studied at 0.025 M imidazole and 5 °C, and the plot of $\ln k_{obsd.}$ vs. pressure gave a good linear fit from which the value of $\Delta V^{\ddagger}$ was calculated to be −12.9±0.3 $cm^3{\cdot}mol^{-1}$. The results are summarized in Table 5. The reported activation parameters favour an associative interchange (I_a) mechanism.

Mechanistic Interpretation

Most ligand substitution reactions of Co^{III} complexes, such as those in vitamin B_{12}, its derivatives and model complexes, follow a D or I_d mechanism.[9−17] Surprisingly, the substitution reactions investigated in the current study between $[Co^{III}(s\text{-}BQDI)_2(Ph_3P)]^+$ and imidazole or 4-Me_2Npy clearly follow an associative mechanism. Simandi et al. studied the ligand substitution reactions of $[Co^{III}(s\text{-}CBQDI)_2(Ph_3As)]^+$ with pyridine, pyrrolidine, and imidazole in methanol and suggested an I_a mechanism, but no activation parameters were reported.[3]

The second-order rate constant for the reaction between $[Co^{III}(s\text{-}BQDI)_2(Ph_3P)]^+$ and imidazole in methanol at 25 °C ($4.5{\cdot}10^{-4}$ $M^{-1}{\cdot}s^{-1}$) is significantly smaller than that obtained in the case of CH_3CN as solvent ($1.78{\cdot}10^{-2}$ $M^{-1}{\cdot}s^{-1}$). This suggests either that hydrogen bonding plays an important role in methanol as solvent by deactivating the attacking nucleophile, or that the stronger donor properties of acetonitrile labilizes the *trans* position and induces a rapid displacement of phosphane.

The rates of associative substitution reactions can in principle be affected by the nature of the solvent. Especially in the case of protic solvents, partial protonation of the nucleophile, directly or through hydrogen bonding, can cause a significant decrease in the nucleophilicity of the entering nucleophile. Specific solvation of the nucleophile by a protic solvent strongly stabilizes the nucleophile and lowers its reactivity toward an electrophilic metal centre in an associative reaction mode. In contrast, polar non-protic solvents such as acetonitrile favour associative reaction modes.[8]

In the case of the benzosemiquinonediimine chelate, delocalization of electron density from the unsaturated equatorial ligand (s-BQDI) onto the Co^{III} centre could partially induce Co^{II} character, which could in turn account for the higher liability and the observed associative mechanism. The strongly negative activation entropies and volumes support the associative nature of the substitution mechanism for these complexes. By way of comparison, in complexes of ethylenediamine, the chelate is fully saturated and an I_d mechanism is more likely to account for the observed kinetic behaviour. It seems clear that the phenylenediamine ligand in the equatorial plane controls the ligand displacement mechanism. The induced electron density at the metal centre favours the unsaturated five-coordinate state and lowers the energy barrier to bind the entering nucleophile in the absence of a strongly coordinating solvent to favour the associative reaction pathway. In the presence of a more strongly coordinating solvent such as acetonitrile, the absence of a vacant coordination site will force the system to follow an interchange substitution mechanism.

Experimental Section

Materials: All chemicals were of p.a. grade and were used as received. Imidazole was purchased from Aldrich and 4-dimethylaminopyridine was purchased from Across. $[Co(s\text{-}BQDI)_2(Ph_3P)]ClO_4{\cdot}0.5C_6H_6$ was prepared as described previously[5] by treatment of $Co(ClO_4)_2{\cdot}6H_2O$ with *o*-phenylenediamine and triphenylphosphane in the presence of oxygen. The complex was characterised by elemental analysis and by IR and NMR spectroscopy, and the results were in agreement with those reported in the literature.[5]

Instrumentation: UV/Vis spectra and kinetic measurements were recorded in thermostatted cell compartments of Shimadzu UV-2101 and Cary 5 spectrophotometers. Measurements at high pressures were carried out by use of the Shimadzu spectrophotometer equipped with a home-made high-pressure unit.[18] For faster reactions a high pressure, stopped-flow instrumentation was used.[19] Kinetic data were analysed with the OLIS KINFIT programme. All instruments used were thermostatted to the desired temperature (±0.1 °C). Kinetic measurements were carried out under pseudo-first order conditions (i.e., the ligand concentration was in at least a tenfold excess).

Acknowledgments

The authors gratefully acknowledge financial support from the Deutsche Forschungsgemeinschaft, a fellowship from the Alexander von Humboldt foundation (M. S. A. H.), and sabbatical leave from the Ain Shams University, Cairo (M. S. A. H.).

[1] S. M. Peng, C. T. Chen, D. S. Liaw, C. I. Chen, Y. Wang, *Inorg. Chim. Acta* **1985**, *101*, L31−L33.
[2] L. F. Warren, *Inorg. Chem.* **1977**, *16*, 2814−2819.
[3] L. I. Simandi, S. Nemeth, *Inorg. Chim. Acta* **1998**, *270*, 326−329.
[4] A. L. Balch, R. H. Holm, *J. Am. Chem. Soc.* **1966**, *88*, 5201−5209.
[5] S. Nemeth, L. I. Simandi, G. Argay, A. Kalman, *Inorg. Chim. Acta* **1989**, *166*, 31−33.
[6] S. Nemeth, L. I. Simandi, *Inorg. Chem.* **1994**, *33*, 5964−5966.
[7] M. S. A. Hamza, R. van Eldik, P. L. S. Harper, J. M. Pratt, E. A. Betterton, *Eur. J. Inorg. Chem.* **2002**, 580−583.
[8] J. McMurry, *Organic Chemistry*, 2nd ed., Brooks/Cole, California, USA, **1988**.
[9] B. M. Alzoubi, M. S. A. Hamza, C. Dücker-Benfer, R. van Eldik, *Eur. J. Inorg. Chem.* **2002**, 968−974.
[10] G. Stochel, R. van Eldik, *Inorg. Chem.* **1990**, *29*, 2075−2077.
[11] F. F. Prinsloo, M. Meier, R. van Eldik, *Inorg. Chem.* **1994**, *33*, 900−904.
[12] M. Meier, R. van Eldik, *Inorg. Chem.* **1993**, *32*, 2635−2639.
[13] F. F. Prinsloo, E. L. J. Breet, R. van Eldik, *J. Chem. Soc., Dalton Trans.* **1995**, 685−688.
[14] H. M. Marques, *J. Chem. Soc., Dalton Trans.* **1991**, 339−341.
[15] H. M. Marques, J. C. Bradley, L. A. Campbell, *J. Chem. Soc., Dalton Trans.* **1992**, *13*, 2019−2027.
[16] H. M. Marques, J. C. Bradley, K. L. Brown, H. Brooks, *J. Chem. Soc., Dalton Trans.* **1993**, *23*, 3475−3478.
[17] M. S. A. Hamza, C. Dücker-Benfer, R. van Eldik, *Inorg. Chem.* **2000**, *39*, 3777−3783.
[18] M. Spitzer, F. Gartig, R. van Eldik, *Rev. Sci. Instrum.* **1988**, *59*, 2092−2093.
[19] R. van Eldik, W. Gaede, S. Wieland, J. Kraft, M. Spitzer, D. A. Palmer, *Rev. Sci. Instrum.* **1993**, *64*, 1355−1357.

Received February 23, 2003

